

X-ray Crystal Structure of Triaquacopper(II) Dihydrogen 1,2,4,5- Benzenetetracarboxylate Trihydrate and Raman Spectra of Cu^{2+} , Co^{2+} , and Fe^{2+} Salts of 1,2,4,5-Benzenetetracarboxylic (Pyromellitic) Acid

Renata Diniz,^[a] Heitor A. de Abreu,^[a] Wagner B. de Almeida,^[a] Maria T. C. Sansiviero,^[a] and Nelson G. Fernandes*^[a]

Keywords: Hydrogen bonds / X-ray diffraction / Raman spectroscopy / Transition metals

Some transition metal salts (Fe^{2+} , Co^{2+} , and Cu^{2+}) of 1,2,4,5-benzenetetracarboxylic acid (pyromellitic acid) have been synthesized: hexaaquairon(II) dihydrogen 1,2,4,5-benzenetetracarboxylate (**I**), hexaaquacobalt(II) dihydrogen 1,2,4,5-benzenetetracarboxylate (**II**), triaquacopper(II) dihydrogen 1,2,4,5-benzenetetracarboxylate trihydrate (**III**), and triaquacopper(II) 1,2,4,5-benzenetetracarboxylate tetrahydrate (**IV**). Single-crystal X-ray diffraction analysis of compound **III** has been performed. It crystallizes in the non-centrosymmetric space group Pn with two molecules per unit cell. Cu^{2+} and the ligand form an infinite linear chain. The metal atom is coordinated to five O atoms (three of the aqua ligand and two of the pyromellitate ligand) in a distorted trigonal-bipyramidal coordination. The carboxylic groups are involved in two medium intermolecular hydrogen bonds with water molecules. The $\text{O}\cdots\text{O}$ distances are 2.629(5) and 2.639(5) Å. The absolute structure parameter shows that the

crystal and the atomic coordinate sets have the same polarity. Raman spectra of all the compounds and deuterated analogues of Fe^{2+} and Co^{2+} salts are reported. Spectral differences have been observed in the spectra of the compounds that present short hydrogen bonds ($\text{O}\cdots\text{O}$ distance less than 2.5 Å) in comparison to compounds that do not. In the crystal of compounds **I** and **II**, intramolecular short hydrogen bonds are present. Symmetric and asymmetric stretching vibrations of a short intramolecular hydrogen bond are observed at 307 and 874 cm^{-1} in salts **I** and **II**, respectively. The crystal structures of compounds **III** and **IV** do not show short hydrogen bonds, these bands are therefore not observed. These vibrational modes are tentative assignments by deuterium compounds and ab initio calculations of the dihydrogen pyromellitate ion.

(© Wiley-VCH Verlag GmbH, 69451 Weinheim, Germany, 2002)

Introduction

In general, a hydrogen bond, $\text{X}-\text{H}\cdots\text{Y}$ represents a relatively weak inter- or intramolecular interaction in which a positively charged hydrogen atom covalently bonded to X (the proton donor) is further attracted by a negative charge around Y (the proton acceptor). In most cases, the hydrogen atom in a hydrogen bond is more strongly bonded to one particular atom to form a clearly asymmetric hydrogen bond. Typically X and Y are electronegative elements such as N, O, F, Cl, etc. On the other hand, as the interaction $\text{H}\cdots\text{Y}$ becomes stronger, the $\text{X}-\text{H}$ bond is successively elongated. Therefore, the $\text{H}\cdots\text{Y}$ distance becomes shortened and the hydrogen atom seems to be similarly attracted to both of them. In this situation, the donor–acceptor concept is not so clear. Anyhow, when a hydrogen bond is formed the contact between $\text{X}\cdots\text{Y}$ becomes closer than the sum of their van der Waals radii.^[1] The hydrogen bond may

be classified as: 1) strong, when the $\text{X}\cdots\text{Y}$ distance is short and the hydrogen atom is similarly attracted to X and Y atoms; 2) moderate, when the H atom is clearly bonded to X and electrostatically attracted to Y; 3) weak, when the $\text{H}\cdots\text{Y}$ interaction is weak, such that, the $\text{X}\cdots\text{Y}$ distance becomes long. For $\text{X} = \text{Y} = \text{oxygen atom}$, from the crystallographic point of view, the hydrogen bond is weak when the $\text{O}\cdots\text{O}$ distance is around 2.8–3.0 Å. The hydrogen bond is moderate when the $\text{O}\cdots\text{O}$ distance is somewhere between 2.5–2.8 Å and a hydrogen bond is short when the $\text{O}\cdots\text{O}$ distance is about 2.4–2.5 Å.

This work is part of a project involving crystallographic and spectroscopic studies of substances containing short hydrogen bonds (SHB). The 1,2,4,5-benzenetetracarboxylic acid, also known as pyromellitic acid [H_4Pm], is a very interesting system to study. At first, it can form different types of coordination compounds, due to the possibility of substitution of one to four hydrogen atoms. Therefore, it is possible to form intramolecular SHB, due to the proximity of the carboxylate and carboxylic groups. Some single-crystal structures of salts of this acid have been reported.^[2–5] In most cases, there are SHB in these acid salt compounds. In Ni^{2+} and Co^{2+} acid salt compounds, two crystalline phases

^[a] Departamento de Química, ICEx, Universidade Federal de Minas Gerais
Av. Antônio Carlos 6627, 31270-901, Belo Horizonte, MG, Brazil
Fax: (internat.) + 55-33/3499-5700
E-mail: nelsongf@apolo.qui.ufmg.br

have been identified. SHB have been observed in both phases. From the crystallographic point of view, in one phase (α) symmetric intramolecular SHB occur and in another phase (β) there are asymmetric intramolecular SHB. In the symmetric SHB, the H atom is located in a glide plane (x , $1/2$, z). These complexes show potential practical interest such as detergent builders, catalysts, and heat stabilisers. The properties of these salts can be influenced by the presence of four carboxylic groups.^[3] Multi-dentate complexing agents are able to form one-, two-, or three-dimensionally infinite connections between cations and anions. Due to the presence of four carboxylic groups in pyromellitic acid, its salts can coordinate in numerous ways and in different dimensionalities.

Various experimental and theoretical studies have reported on the nature of hydrogen-bonding systems.^[6–8] Infrared spectroscopy has been very important in HB investigations. Spectra of a hydrogen-bonding system present broader, more intense and shifted bands than non-hydrogen-bonding systems.^[6] However, hydrate compounds generally show some broad and intense envelope bands in the range of hydrogen-bond (HB) modes. In contrast, the water modes are very weak in Raman spectra. As a result of this, the Raman spectra of hydrate compounds are usually better than infrared spectra. Reid^[9] interpreted the changes in the infrared spectra by making a semiempirical treatment of the hydrogen bond based on the Lippincott and Schroeder potential.^[10] This treatment considers the coupling between the slow O \cdots O stretching motion with the fast OH vibration. The O \cdots O motion of two hydrogen-bonded oxygen atoms has been investigated much less than the O–H stretching mode, since it is in a range that is extremely difficult to separate from many other vibration modes. Reid used a harmonic oscillator approximation to calculate the O \cdots O stretching frequency with respect to the O \cdots O equilibrium distance. For a short O \cdots O distance (< 2.5 Å), a frequency of ca. 850 cm^{-1} was found. Miller et al.^[11] studied the O–H–O hydrogen bond in $\text{CsH}(\text{CF}_3\text{CO}_2)_2$ and $\text{KH}(\text{CF}_3\text{CO}_2)_2$. These compounds show very short O \cdots O distances. They assigned the O \cdots H \cdots O mode at 798 and 792 cm^{-1} to Cs and K salts, respectively, by Raman spectroscopy. Hadzi, Orel, and Novak^[12] also discussed the Raman and infrared spectra of the $\text{MH}(\text{CX}_3\text{COO})_2$, where $\text{M} = \text{Na}$ or K and $\text{X} = \text{H}$ or F , and they assigned values of 720 and 320 cm^{-1} for the $\nu_{\text{asym}}(\text{OHO})$ and $\nu_{\text{sym}}(\text{OHO})$ bands, respectively. Luehrs et al.^[13] investigated some salts of pyromellitic acid using infrared spectroscopy. They mentioned that an enlargement between 900 and 1800 cm^{-1} could be attributed to the presence of SHB.

In the present work, hydrogen bonds have been investigated in four salts: hexaaquairon(II) dihydrogen 1,2,4,5-benzenetetracarboxylate $\{[\text{Fe}^{2+} \cdot 6\text{H}_2\text{O}][\text{C}_{10}\text{H}_4\text{O}_8]^{2-}\}$ (FeH_2Pm) (**I**); hexaaquacobalt(II) dihydrogen 1,2,4,5 benzenetetracarboxylate $\{[\text{Co}^{2+} \cdot 6\text{H}_2\text{O}][\text{C}_{10}\text{H}_4\text{O}_8]^{2-}\}$ (CoH_2Pm) (**II**), triaquacopper(II) dihydrogen 1,2,4,5-benzenetetracarboxylate trihydrate $\{[\text{Cu} \cdot 3\text{H}_2\text{O}][\text{C}_{10}\text{H}_4\text{O}_8 \cdot 3\text{H}_2\text{O}]\}$ (CuH_2Pm) (**III**); triaquacopper(II) 1,2,4,5-benzenetetracarboxylate tetrahydrate $\{[\text{Cu} \cdot 3\text{H}_2\text{O}]_2\text{C}_{10}\text{H}_2\text{O}_8 \cdot 4\text{H}_2\text{O}\}$ (Cu_2Pm) (**I**).

From powder diffraction data, it can be concluded that FeH_2Pm and CoH_2Pm are isostructural. The crystal structure of CoH_2Pm was reported^[3] earlier. These compounds show intramolecular SHB. The crystal structural investigation of CuH_2Pm is shown in this work and the crystal structure of Cu_2Pm was reported^[2] elsewhere. These last two compounds show moderate intermolecular hydrogen bonds. All of these compounds are hydrated, with compounds **I**, **II**, and **III** having six water molecules in their structures, and compound **IV** showing ten water molecules. Due to this, Raman spectroscopy has been chosen to study spectral differences in short and long/medium HB modes. The SHB modes occur in a crowded region, thus Raman spectra of deuterated analogues of CoD_2Pm and FeD_2Pm have been obtained, and ab initio molecular orbital (MO) calculations have also been performed for the dihydrogen pyromellitate ion $[\text{H}_2\text{Pm}]^{2-}$ with the purpose of SHB mode assignment.

Results and Discussion

Description of Structures

Crystal Structure of CuH_2Pm

The crystal structure of CuH_2Pm is shown in Figure 1. Selected bond lengths and bond angles are listed in Table 1. The coordination number of Cu^{2+} is five, it is coordinated to three water molecules and two carboxyl groups of two ligand molecules $[\text{H}_2\text{Pm}]^{2-}$. The average of the Cu–O bonds is $1.944(2)$ Å to the ligand O atoms and $2.070(4)$ Å to the water molecules. The longest Cu–O bond length is Cu–O11 [$2.235(4)$ Å]. At a first glance, Figure 1 could suggest a square-pyramidal oxygen atom arrangement around Cu^{2+} . The best least-squares plane through O1, Cu, O5ⁱ, O9, and O10 shows that only the metal atom lies in this plane, however, O1, O5ⁱ, O9, and O10 are on average $0.15(2)$ Å below and above that plane. The symmetry code of i is x , $1 + y$, z . On the other hand, the best least-squares plane through the metal ion and the three oxygen atoms of the water molecules is the plane through Cu, O9, O10, and O11. All the atoms lie in this plane with an average distance of $0.005(3)$ Å. Therefore, it can be concluded that the oxygen arrangement around the metal ion is better described as a slightly distorted trigonal-bipyramidal structure. This geometry was observed in the Cu_2Pm crystal structure by Usabalieve et al.^[2] The water molecules form the pyramid base and O–Cu–O angles are $165.4(2)^\circ$ (O9,O10), $94.8(3)^\circ$ (O9, O11), and $99.8(3)^\circ$ (O10, O11). At the top and bottom of the coordination geometry O1 and O5 are attached to the ligand molecule. The average of O–Cu–O angles is $89.5(2)^\circ$ and the O1–Cu–O5 angle is $176.3(2)^\circ$. Cu^{2+} atoms are bonded in a monodentate form to O1 and O5 atoms of different H_2Pm ligands. These O atoms are located on opposite sides of the benzene ring and the Cu^{2+} atoms are linked between ligand molecules. These bonds form an infinite linear chain, as can be seen from Figure 1.

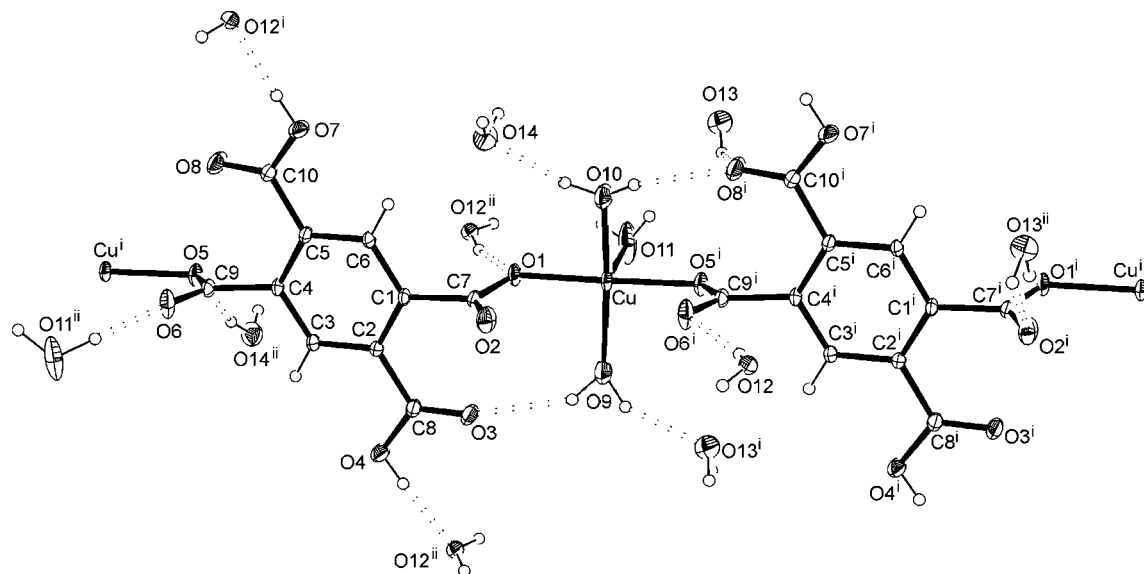


Figure 1. Atomic labelling scheme for CuH_2Pm and displacement ellipsoids with 30% probability level; symmetry codes: *i*: $x, 1 + y, z$; *ii*: $0.5 + x, -y, 0.5 + z$

Table 1. Selected bond lengths and bond angles for CuH_2Pm

Bond lengths [Å]					
Cu–O1	1.939(2)	O1–C7	1.284(5)	O5–C9	1.271(4)
Cu–O5 ⁱ	1.948(2)	O2–C7	1.227(5)	O6–C9	1.236(4)
Cu–O9	1.984(2)	O3–C8	1.213(4)	O7–C10	1.307(4)
Cu–O10	1.990(4)	O4–C8	1.314(4)	O8–C10	1.211(4)
Cu–O11	2.235(4)				
Bond angles [°]					
O1–Cu–O5 ⁱ	176.3(2)	O5–Cu–O9	91.4(2)	O9–Cu–O11	94.8(3)
O1–Cu–O9	88.7(2)	O5–Cu–O10	90.6(2)	O10–Cu–O11	99.8(3)
O1–Cu–O10	90.2(2)	O5–Cu–O11	84.8(1)	C7–O1–Cu	119.7(2)
O1–Cu–O11	91.4(2)	O9–Cu–O10	165.4(2)	C9–O5–Cu	114.3(2)
Hydrogen bonds					
D–H···A	Distance D–A [Å]	Bond angles [°]	D–H···A	Distance D–A [Å]	Bond angles [°]
O4–H4A–O12 ⁱⁱ	2.639(5)	175.9(4)	O11–H11A–O6 ⁱⁱ	2.757(7)	170.4(4)
O7–H7A–O12 ⁱ	2.629(5)	172.6(4)	O12–H12A–O1 ⁱⁱ	2.694(5)	165.7(5)
O9–H9A–O3	2.927(6)	146.6(4)	O12–H12B–O6 ⁱ	2.685(5)	152.1(4)
O9–H9B–O13 ⁱ	2.701(7)	149.1(5)	O13–H13A–O8 ⁱ	3.000(6)	141.4(4)
O10–H10A–O8 ⁱ	2.905(5)	154.4(4)	O13–H13B–O2 ⁱⁱ	2.891(6)	171.9(5)
O10–H10B–O14	2.731(6)	168.3(6)	O14–H14A–O5 ⁱⁱ	2.975(5)	165.8(5)

In the carboxyl groups the averages of C–O and C=O bonds are 1.294(4) and 1.222(4) Å, respectively. In the carboxylate groups O1–C7–O2 and O5–C9–O6 the difference between C–O and C=O bonds is smaller than usually in carboxylic groups due to the delocalization of the electrons as can be seen in Table 1. The average of the C–C–C, O–C–O, and C–C–O angles is 120(3)°. The benzene ring is planar with a maximum deviation of 0.006 Å. The distances of the carboxyl group atoms to the benzene plane are 0.003(6), 0.009(6), –0.197(7), 0.039(6), 1.175(7), –1.055(6), 0.075(8), –0.058(7), 0.834(7), –1.348(6), 0.183(8), and –0.082(7) Å to C7, C8, C9, C10,

O1, O2, O3, O4, O5, O6, O7, and O8, respectively. The COOH planes are rotated against the mean plane through the benzene ring by –7.1 and –3.2°, and the COO[–] planes are rotated by –87.1 and +95.4°. This conformation is similar to that found in pyromellitic acid (H_4Pm) for which the torsion angles are 17.9 and 74.4°. [14] CuH_2Pm crystallizes in a non-centrosymmetric space group, so the absolute structure could be obtained. The absolute structure parameter x , Flack parameter, may be determined for any non-centrosymmetric crystal. This parameter is a variable in the least-squares refinement. [15] The Flack parameter was refined to 0.01(2). The refined value of x is independent of

the starting values. Therefore, this value indicates that the crystal and atomic coordinates have the same polarity.^[15]

The carboxylic groups present are not involved in SHB. There are three water molecules of crystallization in this structure (O12, O13 and O14). These water molecules are also involved in medium and long hydrogen bonds. The ligand H₂Pm is an acceptor of two medium (O12) and three long (O13 and O14) hydrogen bonds from water molecules. The O12...O1ⁱⁱ, O12...O6ⁱ, O13...O2ⁱⁱ, O13...O8ⁱ, and O14...O5ⁱⁱ distances are 2.694(5), 2.685(5), 2.891(6), 3.000(6), and 2.975(5) Å, respectively. The coordination water molecules are donors to one medium (O11) and two long (O9, O10) hydrogen bonds. The O6ⁱⁱ...O11, O8ⁱ...O10, and O3...O9 distances are 2.757(7), 2.905(5), and 2.927(6) Å, respectively. Two medium hydrogen bonds between the water molecules were observed. The O10...O14 and O9...O13 distances are 2.731(6) and 2.701(7) Å, respectively. The H₂Pm ligand is the donor of two medium hydrogen bonds to waters of crystallization (O12). The O7–O12ⁱ and O4–O12ⁱⁱ distances are 2.629(5) and 2.639(5) Å, respectively. The symmetry code of *ii* is 0.5 + *x*, −*y*, 0.5 + *z*.

Powder Diffraction Data

As described in the Exp. Sect., there was not a suitable single crystal for X-ray analysis of FeH₂Pm. Therefore, powder diffraction methods were used to identify iron compounds. In order to make sure that in the absence of a single crystal, powder diffraction techniques can be useful for identification of a structure type, some X-ray powder patterns are shown in Figure 4. The program XPOW^[16] was used to generate X-ray powder patterns.

CuH₂Pm and Cu₂Pm Structures

The calculated X-ray powder patterns of CuH₂Pm are based on the cell parameters, atomic position, and displacements obtained from single-crystal structure refinement described in this present work. The X-ray powder pattern of Cu₂Pm was obtained from a single-crystal structure by Usabalieve et al.^[2] In Cu₂Pm the water molecules of crystallization are involved in medium and long hydrogen bonds with the ligand. The average O...O distances in medium and long hydrogen bonds are 2.69(1) and 2.85(5) Å, respectively. Cu₂Pm forms two cross infinite chains, where the Cu²⁺ is the link between the ligand molecules (Figure 2). Cu²⁺ shows the same coordination geometry as CuH₂Pm. The powder patterns are shown in Figure 4 (a).

CoH₂Pm and FeH₂Pm

There are two crystal phases reported for the Co²⁺ salt.^[3,5] In both of them there are intramolecular SHB, and Co²⁺ is coordinated by six water molecules in an octahedral geometry. The carboxyl groups are involved in a short intramolecular hydrogen bond with an O...O distance of about 2.4 Å. From a crystallographic point of view, one of these phases (*α*) shows symmetric intramolecular SHB^[3] and the other (*β*) shows asymmetric SHB.^[5] The *α* phase crystal

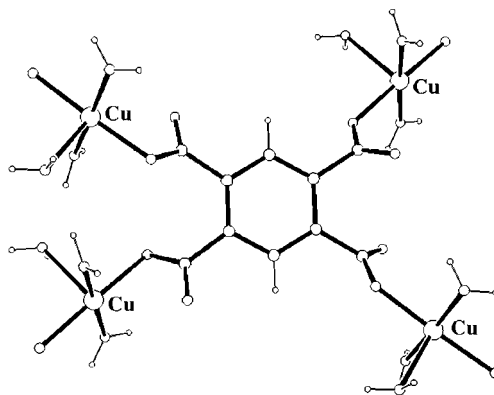


Figure 2. Crystal structure of Cu₂Pm

structure is shown in Figure 3. In the symmetric SHB, the H atom is located in a glide plane (*x*, 1/2, *z*). In the *α* phase the carboxyl groups are coplanar with the benzene ring while in the *β* phase the dihedral angles of the carboxyl group with the benzene ring are about 25°. In Figure 4 (b), experimental (Co²⁺ and Fe²⁺ salts) and calculated (*α* and *β* phase) X-ray powder patterns are shown. For the *α* phase the calculated pattern was obtained from single-crystal data by Ward and Luehrs.^[3] For the *β* phase the calculated powder pattern has been performed from single-crystal data given by Rochon and Massarweh.^[5]

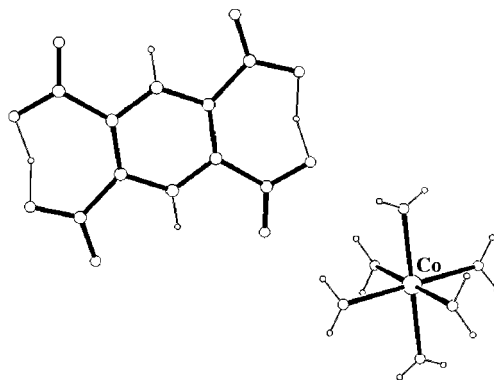


Figure 3. Crystal structure of the *α* phase of CoH₂Pm

Experimental FeH₂Pm and CoH₂Pm X-ray powder patterns are very similar, therefore, it can be concluded that they may be isostructural. This similarity shows that the Fe²⁺ and Co²⁺ salts obtained in this work have the same structure as the Co²⁺ salt published by Ward and Luehrs.^[3]

Raman Spectroscopy and Vibrational Mode Assignment

Experimental Raman spectra of the compounds and a theoretical Raman spectrum of the H₂Pm^{2−} ion are displayed in Figures 5 and 6, and its deuterated counterpart for Fe²⁺ and Co²⁺ salts are shown in Figure 7. The Raman frequencies are shown in Tables 2 and 3.

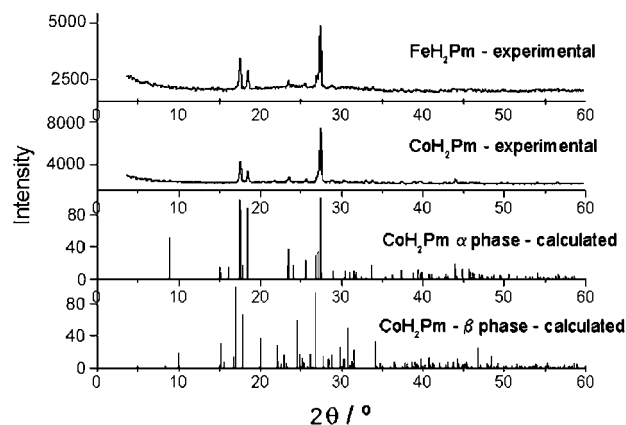
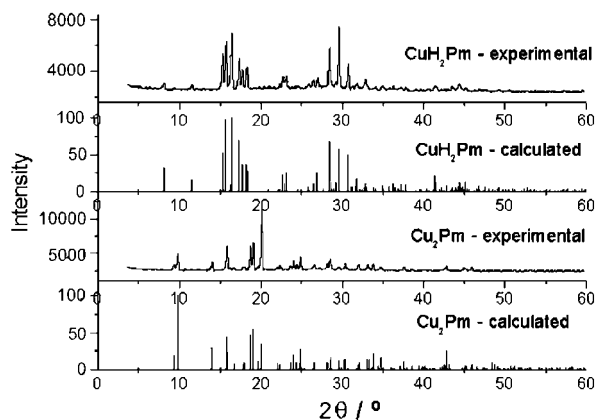


Figure 4. Experimental and calculated powder patterns of a) Cu_2Pm and CuH_2Pm and b) FeH_2Pm and CoH_2Pm

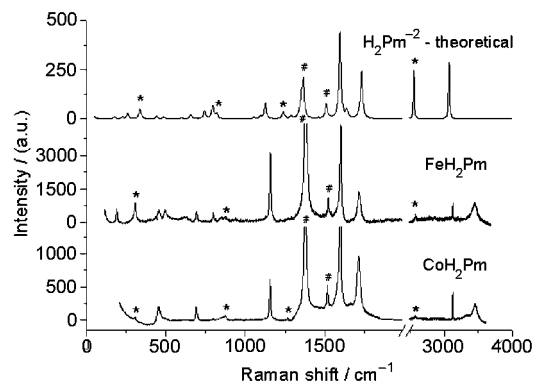


Figure 5. Raman spectra of Fe^{2+} and Co^{2+} salts of pyromellitic acid; the symbol * refers to bands relative to SHB vibrations; The symbol # refers to $\nu_{\text{sym}}(\text{COO})$ and $\nu_{\text{asym}}(\text{COO})$

Carboxyl Modes

The stretching vibration of carboxyl groups is easily assigned as they are very intense and appear in a characteristic region. There are two stretching vibrations for the carboxylate group, one symmetric [$\nu_{\text{sym}}(\text{COO})$] and another asymmetric [$\nu_{\text{asym}}(\text{COO})$]. In CoH_2Pm and in FeH_2Pm the $\nu_{\text{sym}}(\text{COO})$ and $\nu(\text{C}=\text{O})$ are strongly coupled with $\delta(\text{OH})$.

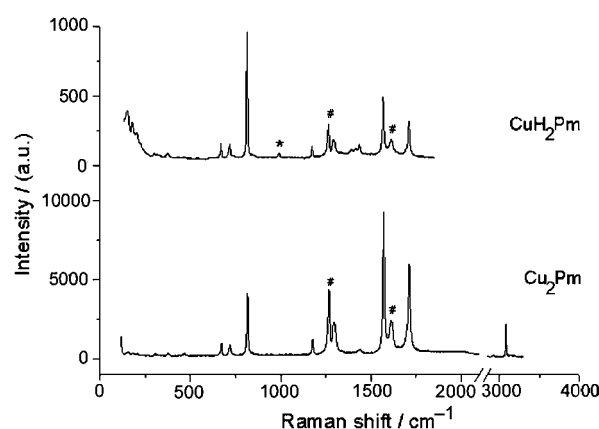


Figure 6. Raman spectra of copper salts of pyromellitic acid; the symbol * refers to $\gamma(\text{OH})$; the symbol # refers to $\nu_{\text{sym}}(\text{COO})$ and $\nu_{\text{asym}}(\text{COO})$

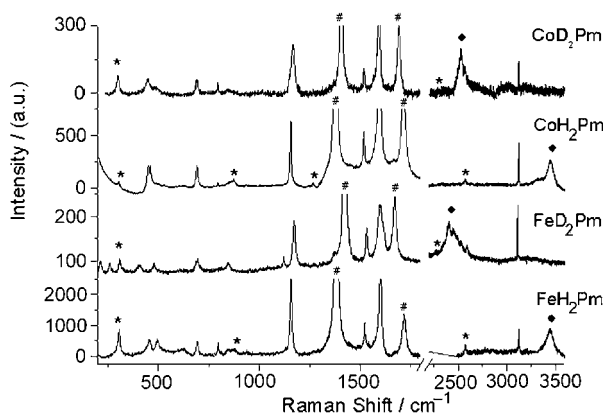


Figure 7. Raman spectra of the SHB region of FeH_2Pm , CoH_2Pm and deuterated analogues; the symbol * refers to bands relative to SHB vibrations; the symbol # refers to $\nu_{\text{sym}}(\text{COO})$ and $\nu(\text{C}=\text{O})$; the symbol ♦ refers to $\nu[\text{OH}(\text{D})]$ from $\text{H}(\text{D})_2\text{O}$

These couplings were confirmed by ab initio calculations and by the frequency shift of these bands in the Raman spectra of the deuterated analogues. In the CoH_2Pm salt the $\nu_{\text{sym}}(\text{COO})$ and $\nu(\text{C}=\text{O})$ were observed at 1378 and 1714 cm^{-1} , respectively, and they shift to 1406 and 1691 cm^{-1} after deuteration. Similar shifts were observed in the Fe^{2+} salt, $\nu_{\text{sym}}(\text{COO})$ and $\nu(\text{C}=\text{O})$ at 1381 and 1718 cm^{-1} respectively, and they shift to 1423 and 1670 cm^{-1} , respectively in the deuterated salt. These strong couplings and shifts were also observed in some hydrogen acetate salts.^[12] The X-ray crystal data of CuH_2Pm show that Cu^{2+} is monodentately coordinated to the carboxylate groups of H_2Pm^{2-} and the carboxylic groups are involved in medium hydrogen bonds to water molecules, as seen in Figure 1. The $\nu_{\text{sym}}(\text{COO})$ and $\nu_{\text{asym}}(\text{COO})$ of the carboxylate groups were observed at 1260 and 1613 cm^{-1} . The $\nu(\text{C}=\text{O})$ for carboxylic groups was assigned at 1318 cm^{-1} and $\nu(\text{C}=\text{O})$ at 1694 and 1711 cm^{-1} . In Cu_2Pm , the $\nu_{\text{sym}}(\text{COO})$ and $\nu_{\text{asym}}(\text{COO})$ were observed at 1268 and 1611 cm^{-1} respectively, and the $\nu(\text{C}=\text{O})$ at 1698 and 1713 cm^{-1} . In-plane bending [$\delta(\text{COO})$] occurs at 796, 798, 817, and 814 cm^{-1} for CoH_2Pm , FeH_2Pm , CuH_2Pm , and Cu_2Pm respectively, and

Table 2. Experimental Raman frequencies for FeH₂Pm and CoH₂Pm and theoretical Raman frequencies for the H₂Pm²⁻ ion

FeH ₂ Pm	Frequency [cm ⁻¹] ^[a] CoH ₂ Pm	H ₂ Pm ²⁻	Tentative assignment
298 m		258	δ(φ)
307 w (300)	307 w (309)	337	v _{sym} (O...H...O)
		441	γ(C=C)
384 m	364 vw		v(M–O)
495 w		485	γ(C=C)
694 w	692 m	684	δ(φ)
798 w	796 vw	743	δ(COO)
845 wb	854 wb	797	γ(COO)
874 wb	874 wb	822	v _{asym} (O...H...O)
	1267 vw (993)	1240	γ(OH)
1381 vs (1423)	1378 vs (1406)	1366	v _{sym} (COO) + δ(OH)
1522 m	1517 m	1510	v _{asym} (COO)
1601 vs	1599 vs	1597	v(C=C)
1718 m (1670)	1714 m (1691)	1733	v(C=O) + δ(OH)
2575 vw	2577 vw	2551	v(O–H) _{HB}
3124 m	3121 m	3066	v(C–H)
3192 m	3197 m	3072	v(C–H)
3444 mb (2400)	3450 mb (2525)		v(O–H) _F

[a] v_{asym} – asymmetric stretching, v_{sym} – symmetric stretching, δ – deformation in plane, γ – deformation out of plane, φ – benzene ring deformation, HB – hydrogen bond, F – free hydrogen group, vw – very weak, w – weak, m – medium, ms – medium strong, s – strong, vs – very strong. Frequencies of deuterated salts are in parentheses.

Table 3. Raman frequencies for copper salts of pyromellitic acid

Cu ₂ Pm	Frequency [cm ⁻¹] ^[a] CuH ₂ Pm	Tentative assignment
377 vw	375 vw	v(Cu–O)
672 w	670 w	δ(φ)
720 w	713 w	δ(φ)
817 ms	814 vs	δ(COO)
	991vw	γ(OH)
1177 w	1175 w	δ(C–H)
1268 m	1260 m	v _{sym} (COO)
1296 m	1288 w	v(C=C)
1297 m	1293 w	v(C=C)
	1318 w	v(C–O)
	1415 w	v(C=C)
1437 vw	1437 w	v(C–O)
1571 vs	1568 ms	v(C=C)
1611 m	1613 m	v _{asym} (COO)
1698 w	1694 w	v(C=O)
1713 s	1711 m	v(C=O)
3081 m		v(C–H)
3143 m		v(O–H) _F

[a] v_{asym} – asymmetric stretching, v_{sym} – symmetric stretching, δ – deformation in plane, γ – deformation out of plane, φ – benzene ring deformation, HB – hydrogen bond, F – free hydrogen group, vw – very weak, w – weak, m – medium, ms – medium strong, s – strong, vs – very strong. Frequencies of deuterated salts are in parentheses.

out-of-plane bending [γ(COO)] was observed at 854 and 845 cm⁻¹ for CoH₂Pm and FeH₂Pm. The difference (Δ) between symmetric and asymmetric carboxylate stretching vibrations can be used as a parameter to identify the coor-

dination type. In FeH₂Pm and CoH₂Pm the Δ values are 141 and 139 cm⁻¹, respectively, and in Cu²⁺ salts Δ is about 343 cm⁻¹. The crystal data show that Cu²⁺ has monodentate coordination, while Fe²⁺ and Co²⁺ do not coordinate to the dihydrogen pyromellitate ion. These results are in agreement with those of acetate compounds,^[17] for which the Δ value is larger in monodentate complexes than in the free ion.

Benzene Ring and M–O Modes

The assignments for the aromatic ring moiety were based on that for substituted benzene^[18,19] and are listed in Tables 2 and 3. The M–O stretching modes were observed at about 375 and 377 cm⁻¹ for CuH₂Pm and Cu₂Pm, and 384 and 364 cm⁻¹ to FeH₂Pm and CoH₂Pm respectively.^[20]

O–H Modes

Crystal data shows that in the crystal structure of the Cu²⁺ salts SHB are not present, while in both Fe²⁺, and Co²⁺ salts there are intramolecular SHB. In FeH₂Pm and CoH₂Pm, the O–H stretching of the carboxylic group was observed at 2575 and 2577 cm⁻¹, respectively. For free OH this mode occurs at 3700 cm⁻¹. These shifts to lower frequencies of the O–H carboxylic stretching are due to the formation of SHB. In the deuterated analogues, the v(O–D) of SHB may be tentatively assigned to a very weak band at 2300 cm⁻¹ in the Co²⁺ salt and at 2359 cm⁻¹ in the Fe²⁺ salt. The v_{OH}/v_{OD} ratios are 1.12 and 1.09, respectively, for Co²⁺ and Fe²⁺ salts. The O–H stretching of water molecules was observed at 3143 cm⁻¹ for Cu₂Pm, at 3444 cm⁻¹ for FeH₂Pm, and 3450 cm⁻¹ for CoH₂Pm. The v(O–D) of water molecules are assigned to a very broad band near 2525 and 2400 cm⁻¹ for Co²⁺ and Fe²⁺ salts, respectively. The v_{OH}/v_{OD} ratios are 1.36 and 1.44 for Co²⁺ and Fe²⁺ salts, respectively. These ratios are in agreement with the isotopic substitution effect. The γOH mode is very weak in Raman spectra and was only observed in CoH₂Pm and CuH₂Pm at 1267 and 991 cm⁻¹, respectively. In deuterated salts, the γOD could not be assigned.

O...H...O Modes

The SHB stretching modes in the FeH₂Pm and CoH₂Pm were tentatively assigned to very broad and weak bands at 874 cm⁻¹ for the asymmetric stretching mode [v_{asym}(O...H...O)], and at 307 cm⁻¹ for the symmetric mode [v_{sym}(O...H...O)] in both salts. These tentative assignments are in accordance with the semiempirical treatment of the hydrogen bond.^[9] As these regions have many modes, tentative assignments were made using deconvolution methods, isotopic substitution (OH/OD) and ab initio calculations for H₂Pm²⁻. Although ab initio calculations have been done in the gaseous phase and without a metallic cation, their results are in agreement with solid-state data. The dihydrogen pyromellitate ion (H₂Pm) is not coordinated to metallic Fe²⁺ and Co²⁺, thus the crystal packing is more important for geometric and vibrational changes than metal coordination. The starting point of the ab initio calcula-

tions was the X-ray crystal structure of the CoH_2Pm α phase,^[3] which minimises differences between theoretical (gaseous phase) and experimental (solid phase) data due to crystal packing. In ab initio calculations the symmetric and asymmetric stretching modes were obtained at 337 and 822 cm^{-1} , respectively.

In Raman spectra, the $\nu_{\text{sym}}(\text{O}\cdots\text{H}\cdots\text{O})$ mode is symmetric about the H atom. The hydrogen atom does not move and no frequency shift due to mass difference is expected upon deuteration.^[11] In the deuterated analogues, the $\nu_{\text{sym}}(\text{O}\cdots\text{D}\cdots\text{O})$ was observed at 309 and 300 cm^{-1} for Co^{2+} and Fe^{2+} salts, respectively. In CoH_2Pm and FeH_2Pm , the $\nu_{\text{asym}}(\text{O}\cdots\text{H}\cdots\text{O})$ was tentatively assigned to 874 cm^{-1} . As this region is crowded and SHB modes become a little broader in deuterated analogues, the assignment becomes more difficult. On the other hand, it is known that deuteration causes little shift in asymmetric O–H–O stretching as was observed in the infrared spectra of potassium hydrogen maleate^[21] and lithium hydrogen phthalate monohydrate.^[22] In contrast, in Cu^{2+} salts, which do not show any SHB, similar bands were not observed in these regions.

The $\nu(\text{O}\cdots\text{H}\cdots\text{O})$ of long and medium hydrogen bonds are expected at low frequencies (about 120 cm^{-1}). However, this region has lattice and hydrogen-bond water modes, which makes it difficult to assign the $\text{O}\cdots\text{H}\cdots\text{O}$ mode.

Computations

Vibrational modes of the short hydrogen bond occur in regions where there are other Raman-active modes. In this work, quantum-mechanical calculations were used in an attempt to observe and assign those specific hydrogen-bond modes.

Geometry optimization and frequency calculations were made for H_2Pm^{2-} with intramolecular SHB. The starting point of the geometry calculations was the α phase of CoH_2Pm , as described by Ward and Luehrs.^[3] In spite of

the fact that the calculations have been performed in the gas phase, they are in good agreement with the experimental values of the Co^{2+} salt.^[3] Table 4 contains both theoretical and experimental geometric parameters for H_2Pm^{2-} . This good agreement between experimental and theoretical data is due to the fact that in the crystal structure of the α -phase CoH_2Pm , Co^{2+} does not coordinate to H_2Pm^{2-} , therefore it is an ionic compound. Co^{2+} is coordinated to six water molecules in an octahedral geometry. There is a weak interaction between H_2Pm^{2-} and coordinated water molecules. H_2Pm^{2-} is the receptor of three long hydrogen bonds involving the water molecules. This is a weak interaction, therefore the greatest difference between the crystal and the gaseous phase is the crystal packing. However, the geometry optimization was performed using the coordinates of the crystal structure, which reduce crystal packing effects. As a result, theoretical and experimental data, geometry and frequency calculations and X-ray crystal data and the Raman spectrum of the ionic salt CoH_2Pm , could be compared and were similar.

The maximum deviations between theoretical and experimental data were 2 and 6%, respectively, for angles and bond lengths. The computed C–C bonds and C–C–C angles are in excellent agreement with experimental values. The computed O···O distance for a short symmetric intramolecular hydrogen bond (2.336 Å) is in good agreement with the experimental value (2.381 Å). The experimental C–Obond values are larger than the computed ones, and the carboxyl groups are more planar. This occurs due to the fact that in the crystal structure the water coordination molecules are involved in medium hydrogen bonds with carboxyl groups. The frequency calculations are listed in Tables 2 and 3. The simulated and experimental Raman spectra of the compounds are shown in Figure 4. Theoretical wavenumbers listed in Table 2 are multiplied by a scale factor of 0.8929. This scale factor is an average from the comparison of several computed and experimental data.^[23]

The frequencies (ν_i) and the vibrational intensities (A_i), obtained in the ab initio calculation, were fitted to a Lorentzian-type function to describe the vibrational spectra. In this process, the concentration was considered equal to $c = 1 \cdot 10^{-3}$ in the Raman spectrum where $l = 1$ cm. To simplify the procedure, a constant value for the full width at half maximum (ω) was considered in all spectral regions, $\omega = 15 \text{ cm}^{-1}$. Equation (1) represents the absorbance for a given frequency, ν .

$$A(\nu) = \left[\ln \left(\frac{I_0}{I} \right) \right]_{\nu} = c l \sum_{i=1}^{3N-6} \left[A_i \left(\frac{2\omega_i}{\pi} \right) \right] \cdot \left\{ \frac{1}{4(\nu - \nu_i)^2 + \omega} \right\} \quad (1)$$

The theoretical Raman spectrum of H_2Pm^{2-} is very similar to the spectra of Fe^{2+} and Co^{2+} salts. The short hydrogen-bond modes were obtained at 822 for $\nu_{\text{asym}}(\text{O}\cdots\text{H}\cdots\text{O})$, and 337 for $\nu_{\text{sym}}(\text{O}\cdots\text{H}\cdots\text{O})$. The relative deviations of experimental data were 5.9 and 9.8%, respectively. In the fre-

Table 4. Bond lengths and bond angles of dihydrogen pyromellitate ion – experimental and calculation data

	Exp. ^[3]	Calcd.
Distances [Å]		
C1–C2	1.394(1)	1.392
C2–C2'	1.414(2)	1.408
C2–C3	1.522(1)	1.538
C3–O1	1.286(1)	1.211
C3–O2	1.299(1)	1.274
Angles [°]		
C2–C1–C2'	124.76(6)	124.36
C1–C2–C2'	117.64(7)	117.83
C1–C2–C3	113.66(10)	114.31
C2'–C2–C3	128.69(5)	127.87
C2–C3–O1	118.97(9)	118.22
C2–C3–O2	119.92(9)	117.77
O1–C3–O2	121.09(8)	123.97
C1–C2–C3–O1	2.01(15)	–15.79
C2'–C2–C3–O2	–176.56(10)	–18.4

quency calculations, a shift to low frequencies was observed for the O–H stretching of the carboxylic group (2551 cm^{-1}). This stretching is very sensitive to hydrogen-bond interactions and is in good agreement with the experimental data (2575 cm^{-1}). The O–H deformation modes were obtained at 1054 and 1539 cm^{-1} for out-of-plane and in-plane, respectively. Theoretical benzene ring deformation modes are strongly coupled with C–H and COO deformation modes.

Conclusion

Although the vibrational modes of hydrogen bonds are weak in Raman spectroscopy, it was possible to carry out a study of these types of interactions. The $\text{O}\cdots\text{H}\cdots\text{O}$ modes lie in a crowded region of the spectrum, but these modes were identified and tentatively attributed with the aid of deconvolution techniques, isotopic substitution and ab initio calculations. The optimized geometry in the gas phase is in good agreement with the experimental X-ray crystal data. Information about different types of hydrogen bonds (short or long) can be obtained using Raman spectroscopy.

FeH_2Pm and CoH_2Pm have a very short intramolecular hydrogen bond with an $\text{O}\cdots\text{O}$ distance of about 2.4 \AA . The short hydrogen bond stretching observed in the Raman spectra was tentatively assigned to a broad band of weak intensity at 874 cm^{-1} for the asymmetric mode [$\nu_{\text{asym}}(\text{O}\cdots\text{H}\cdots\text{O})$] and at 307 cm^{-1} for the symmetric [$\nu_{\text{sym}}(\text{O}\cdots\text{H}\cdots\text{O})$] one. In deuterated analogues the $\nu_{\text{sym}}(\text{O}\cdots\text{H}\cdots\text{O})$ band appears not to shift and the $\nu_{\text{asym}}(\text{O}\cdots\text{H}\cdots\text{O})$ band is unfortunately not possible to assign. The evidence of deuteration was observed by the shift in the frequency of $\nu_{\text{sym}}(\text{COO})$ and $\nu(\text{C}=\text{O})$ modes, which are strongly coupled with the $\delta\text{OH}(\text{D})$ mode, and by the shift of the $\nu(\text{OH})$ of water molecules, whose $\nu_{\text{OH}}/\nu_{\text{OD}}$ is 1.36 for CoH_2Pm and 1.43 for FeH_2Pm .

CuH_2Pm crystallizes in the non-centrosymmetric space group Pn . The carboxyl groups of the H_2Pm^{2-} ions form a linear polymeric structure. In this compound, two medium intermolecular hydrogen bonds [$2.639(5)\text{ \AA}$ and $2.629(5)\text{ \AA}$] were observed and in Cu_2Pm , the pyromellitate ion is a receptor of medium hydrogen bonds with water molecules. The $\nu(\text{O}\cdots\text{H}\cdots\text{O})$ of long and medium hydrogen bonds is expected at low frequencies (about 120 cm^{-1}).

Experimental Section

Synthesis: Powders and single crystals of the compounds were obtained by slow concentration of aqueous solutions at room temperature.

Fe^{2+} Salt: To a hot aqueous solution of pyromellitic acid (3.3 mmol ; Aldrich B400-7, 96%), iron powder (3.2 mmol ; Merck 3819, 99.5%) was added. The final solution was heated until the total oxidation of the iron powder had occurred, filtered, and stored at room temperature. A yellow powder was obtained and characterised as hexaaquairon(II) dihydrogen 1,2,4,5-benzenetetracarboxylate (FeH_2Pm). $\text{C}_{10}\text{H}_{16}\text{FeO}_{14}$ (416.08): calcd. C 28.87, H

3.85, Fe 13.42; found C 28.86, H 3.46, Fe 12.64. Its deuterated derivative was obtained by the reaction of metallic iron (powder) with pyromellitic acid and recrystallised from D_2O .

Co^{2+} Salt: To a hot aqueous solution of pyromellitic acid (3.3 mmol ; Aldrich B400-7, 96%), an aqueous solution of cobalt(II) nitrate hexahydrate (2.9 mmol ; Aldrich 23,037-5, 99%) was added. The final solution was filtered and stored at room temperature. Pink crystals were obtained and characterised as hexaaquacobalt(II) dihydrogen 1,2,4,5-benzenetetracarboxylate (CoH_2Pm). $\text{C}_{10}\text{H}_{16}\text{CoO}_{14}$ (412.22): calcd. C 28.65, H 3.82, Co 14.06; found C 28.67, H 3.83, Co 14.04. Its deuterated derivative was obtained by repeated recrystallization of CoH_2Pm in D_2O .

Cu^{2+} Salts: In a hot aqueous solution of pyromellitic acid (3.2 mmol ; Aldrich B400-7 96%), basic copper(II) carbonate (1.6 mmol ; Aldrich 20,789-6) was dissolved. The final solution was filtered and stored at room temperature. Two types of crystals were obtained, one dark blue and the other light blue. The dark blue crystals were characterised as triaquacopper(II) 1,2,4,5-benzenetetracarboxylate tetrahydrate (Cu_2Pm). $\text{C}_{10}\text{H}_{16}\text{Cu}_2\text{O}_{15}$ (503.32): calcd. C 21.55, H 3.95, Cu 22.80; found C 22.04, H 3.38, Cu 26.79. The light blue crystals were characterised as triaquacopper(II) dihydrogen 1,2,4,5-benzenetetracarboxylate trihydrate (CuH_2Pm). $\text{C}_{10}\text{H}_{16}\text{CuO}_{14}$ (423.78): calcd. C 28.34, H 3.78, Cu 15.00; found C 29.56, H 3.61, Cu 14.20.

Powder: X-ray powder patterns were obtained with a Rigaku diffractometer using Cu radiation ($\lambda = 1.541838\text{ \AA}$) with 4° min^{-1} speed.

Raman Spectroscopy: Raman spectra were obtained with a micro-Raman instrument Dilor X-Y triple monochromator equipped with a CCD detector at room temperature. The 514.5 nm line of an argon ion laser was used as the exciting radiation.

Calculation Methods: Ab initio MO calculations were performed with the Gaussian 98 program package^[24] using a Digital workstation. All calculations were carried out at the Hartree–Fock (HF) level. The 6-31++G** basis set with polarised and diffuse functions added to all the atoms was employed. The X-ray structure of the Co^{2+} salt of pyromellitic acid (CoH_2Pm)^[3] was used as a starting point for geometry optimisation, followed by vibrational analysis. These salts are isostructural to FeH_2Pm . The theoretical vibrational spectra were calculated using the SIMULAT program.^[25]

X-ray Crystallographic Study: $\text{C}_{10}\text{H}_{16}\text{CuO}_{14}$, $M = 423.78$, monoclinic, $a = 6.763(1)$, $b = 10.923(1)$, $c = 9.646(1)\text{ \AA}$, $\beta = 91.925(3)^\circ$, $V = 801.58(4)\text{ \AA}^3$, $T = 298\text{ K}$, space group Pn (no. 07), $Z = 2$, $\mu(\text{Mo-K}\alpha) = 13.9\text{ mm}^{-1}$, $d = 1.756\text{ g cm}^{-3}$, 3220 reflections measured, 3085 unique ($R_{\text{int}} = 0.009$) which were used to refine 229 parameters. Final $R(F)$ and $wR(F^2)$ were 0.037 and 0.114, respectively (all data). The crystal was mounted on a four-circle P4 Siemens diffractometer. XSCANS program^[26] was used to refine the unit-cell parameters and to manage the data collection. Analytical absorption, Lorentz and polarisation effects were corrected using JANA'98,^[27] with maximum and minimum transmission of 0.984 and 0.881, respectively. The structure was solved by Patterson methods in a non-centrosymmetric space group with the XS program.^[16] This space group is non-polar, therefore, Cu fractional coordinates were used as the origin. Hydrogen atoms were located from successive Fourier difference maps. Their atomic coordinates were optimised and fixed. Anisotropic displacement parameters were assigned to all non-hydrogen atoms, the structure was refined using SHELXL-93.^[28] An empirical isotropic extinction parameter x was refined, according to the method describe by Larson.^[29] The

structure was drawn by ORTEP-3 for windows.^[30] CCDC-167303 contains the supplementary crystallographic data for this paper. These data can be obtained free of charge at www.ccdc.cam.ac.uk/conts/retrieving.html or from the Cambridge Crystallographic Data Centre, 12, Union Road, Cambridge CB2 1EZ, UK [Fax: (internat.) + 44-1223/336-033; E-mail: deposit@ccdc.cam.ac.uk].

Acknowledgments

We are grateful to Dr. Marcelo Augusto Silva de Oliveira and Dr. Marcos Assunção Pimenta for the Raman spectroscopy data obtained with a micro-Raman spectrometer at the Departamento de Física of the Universidade Federal de Minas Gerais, and to the Centro de Desenvolvimento de Tecnologia Nuclear (CDTN) for providing the D₂O. This work has been supported by the Fundação de Amparo à Pesquisa do Estado de Minas Gerais, FAPEMIG (Grant CEX 1123/90). R. D. and H. A. A. are grateful to the CNPq for providing the graduate fellowship.

- [1] G. A. Jeffrey, *Topics in physical chemistry: An introduction to hydrogen bonding* (Ed.: D. G. Truhlar), New York, Oxford University Press, **1997**.
- [2] B. T. Usubaliev, A. N. Shnulin, K. S. Mamedov, *Koord. Khim.* **1982**, 8, 1532–1538.
- [3] D. C. Ward, D. C. Luehrs, *Acta Crystallogr., Sect. C* **1983**, 39, 1370–1372.
- [4] S. M. Jessen, H. Küppers, *Z. Naturforsch., Teil B* **1992**, 47, 1141–1153.
- [5] F. D. Rochon, G. Massarweh, *Inorg. Chim. Acta* **2000**, 304, 190–198.
- [6] J. Emsley, *J. Chem. Soc. Rev.* **1980**, 9, 91–124.
- [7] W. Qian, S. Krimm, *J. Phys. Chem. A* **1997**, 101, 5825–5827.
- [8] S. M. Jessen, H. Küppers, *J. Mol. Struct.* **1991**, 263, 247–265.
- [9] C. Reid, *J. Chem. Phys.* **1959**, 30, 182–190.
- [10] E. R. Lippincott, R. Schroeder, *J. Chem. Phys.* **1955**, 23, 1099–1106.
- [11] P. J. Miller, R. A. Butler, E. R. Lippincott, *J. Chem. Phys.* **1978**, 57, 5451–5456.
- [12] D. Hadzi, B. Orel, A. Novak, *Spectrochim. Acta A* **1973**, 29, 1745–1753.
- [13] D. C. Luehrs, C. B. Cornilsen, C. B. Glover, T. L. Neils, *Inorg. Chim. Acta* **1998**, 145, 81–84.
- [14] F. Takusagawa, K. Hirotsu, A. Shimada, *Bull. Chem. Soc. Jpn.* **1971**, 44, 1274–1278.
- [15] H. D. Flack, *Acta Crystallogr., Sect. A* **1993**, 39, 876–881.
- [16] G. M. Sheldrick, *SHELXTL/PC*, Structure Determination Software Programs, Siemens Analytical X-ray Instruments Inc., Madison, Wisconsin, USA, **1990**.
- [17] G. B. Deacon, R. J. Phillips, *J. Coord. Chem. Rev.* **1980**, 33, 227–250.
- [18] D. W. Scott, J. P. McCullough, W. N. Hubbard, J. F. Messerly, I. A. Hossenlopp, F. R. Frow, G. Waddington, *J. Am. Chem. Soc.* **1956**, 78, 5463–5468.
- [19] D. H. Whiffen, *J. Chem. Soc.* **1956**, 1350–1356.
- [20] K. Nakamoto, *Infrared and Raman Spectra of Inorganic and Coordination Compounds*, 4th ed., John Wiley & Sons, New York, **1986**, pp. 229.
- [21] M. M. Ilczyszyn, J. Baran, H. Ratajczak, A. J. Barnes, *J. Mol. Struct.* **1992**, 270, 499–515.
- [22] M. M. Ilczyszyn, A. J. Barnes, H. Ratajczak, *J. Mol. Struct.* **1993**, 291, 135–143.
- [23] A. P. Scott, L. Radom, *J. Phys. Chem.* **1996**, 100, 16502–16513.
- [24] M. J. Frisch, G. W. Trucks, H. B. Schlegel, G. E. Scuseria, M. A. Robb, J. R. Cheesman, V. G. Zakrzewski, J. A. Montgomery, R. E. Stratmann, J. C. Burant, S. Dapprich, J. M. Millam, A. D. Daniels, K. N. Kudin, M. C. Strain, O. Farkas, J. Tomasi, V. Barone, M. Cossi, R. Cammi, B. Mennucci, C. Pomelli, C. Adamo, J. Clifford, J. Ochterski, G. A. Peterson, P. Y. Ayala, Q. Cui, K. Morokuma, D. K. Malick, A. D. Rabuck, K. Raghavachari, B. Foresman, J. Cioslowski, J. V. Ortiz, B. B. Stefanov, G. Liu, A. Liashenko, P. Piskorz, I. Komaromi, R. Gomperts, R. L. Martin, D. J. Fox, T. Keith, M. A. Allaham, C. Y. Peng, A. Nanayakkara, C. Gonzalez, M. Challacombe, P. M. W. Gill, B. G. Johnson, W. Chen, M. W. Wong, J. L. Andres, M. Head-Gordon, E. S. Replogle, J. A. Pople, *Gaussian98* (Revision A.1), Gaussian Inc., Pittsburgh, PA, **1998**.
- [25] H. F. Dos Santos, W. B. De Almeida, A. M. G. Do Val, C. Guimarães, *Quím. Nova* **1999**, 22, 732–736.
- [26] Siemens, *XSCANS*, Version 2.1, Siemens Analytical X-ray Instruments Inc., Madison, Wisconsin, USA, **1991**.
- [27] V. Petrick, M. Dusek, *JANA-98*, Crystallographic Computing System, Institute of Physics, Academy of Sciences of Czech Republic, Praha, **1998**.
- [28] G. M. Sheldrick, *SHELXL-93*, Program for Crystal Structure Solution, University of Göttingen, Germany, **1993**.
- [29] A. C. Larson, *Crystallographic Computing* (Ed.: F. R. Ahmed), Munksgaard, Copenhagen, **1970**, pp. 291–294.
- [30] C. K. Johnson, M. N. Burnett, L. J. Farrugia, *ORTEP-3 for Windows*, Version 1.0.2, University of Glasgow, Scotland, **1998**.

Received July 14, 2001

[I01262]